Fabrication of high aspect ratio silicon micro-/nano-pore arrays and surface modification aiming at long lifetime liquid-infused-type self-cleaning function

Nguyen PHAN* and Nobuyuki MORONUKI*
*Tokyo Metropolitan University
6-6 Asahigaoka, Hino-shi, Tokyo 191-0065, Japan
E-mail: phan-nguyenbinh@ed.tmu.ac.jp

Received 16 August 2013

Abstract
This paper discusses a fabrication process of high aspect ratio (AR) silicon micro-/nano-pore structures and modification of their surfaces to improve the function of liquid-infused-type self-cleaning surfaces. The structure and its hydrophobic surface play an important role to hold a special liquid (a lubricant) on the surface tight to produce an intermediate lubricant layer and any liquid drops, including low surface tension liquids such as oil, can slide easily on it. The nanopore structure with an AR as high as 30 was fabricated by etching in a solution of hydrofluoric acid and hydrogen peroxide. This process based on a catalyst reaction of an array of Au islands that was deposited on a silicon substrate through a particle mask. This original hydrophilic surface was changed to hydrophobic one by depositing self-assembled monolayer of octadecyltrichlorosilane to modify the energy balance at the interface of the solid structure, the lubricant, another liquid, and air. Then the lubricant could be well retained. The functional lifetime was evaluated by measuring the liquid residue on the surface after number of liquid dash. It was confirmed that longer lifetime was obtained with higher AR nanopore structure.

Key words: Structured surface, Self-cleaning, Metal-assisted chemical etching, Self-assembled monolayer (SAM), liquid-infused surface, lifetime.

1. Introduction

Structured surfaces can afford various functions. For self-cleaning, fine structures and/or low surface energy material coating have been tried so far. But these surfaces lose the function when they are used in environment having low surface tension liquids (Aruga et al., 2008, Moronuki, 2016a, Tuteja et al., 2007). To overcome this limitation, structured surfaces are infused with a special liquid (a lubricant) to produce an intermediate lubricant layer, and any liquid drops can slide easily on it (Wong et al., 2011). This design is quite different from the design of the solid self-cleaning surfaces that bases on entrapped air in fine structures beneath water drops (Cassie and Baxter, 1945). Beside self-cleaning, the liquid-infused surfaces have other noticeable functions such as anti-icing, non-fouling (Kreder et al., 2016, Cao et al., 2009, Epstein et al., 2012). However they have the problem of short life function because the lubricant is easy to drop off though the initial performance is good. Kim et al. (2013) proved nanostructure is more suitable than microstructure for the lubricant retention under high shear conditions due to the higher roughness, the more uniform lubricant layer, and the stronger capillary force. Thus high aspect ratio (AR) nanostructures, that enhance the roughness while having strong capillary force, can be a solution for long lifetime functionality.

Metal-assisted chemical etching (MACE), site-selective and directional etching of silicon in which noble metal works as a catalyst, is one of promising methods to fabricate such structures (Huang et al., 2011). To produce an ordered structure, patterning of a metal layer becomes critical. Sphere lithography is one of candidates used to deal with the issue. Fine particle assembly was carried out on a silicon substrate to produce a monolayer. This layer was then machined by chemical etching or physical etching to obtain a mask thus the metal pattern and the morphology of MACE structures were well controlled (Huang et al., 2007, Peng et al., 2007, Moronuki et al., 2016b). Here we introduce a simple method,

a monolayer of silica particles can be used as the mask without need of further etching processes. A gold layer can be deposited through this mask to produce an island-like array with regular pitch. After etching in a solution of hydrofluoric acid and hydrogen peroxide (etchant), micro-/nano-pore structures can be obtained. Ideally, high AR structures can be produced by increasing etching time. However, the Au islands can drop off easily when the substrate is dipped in the etchant or due to gas formation during the MACE process. This problem can be solved by using a highly porous Au layer that is suitable for gas escape and a low surface tension etchant (Geyer et al., 2012, Moronuki et al., 2016b).

Original hydrophilic silicon oxide layer of the pore surfaces can be changed to hydrophobic one by depositing self-assembled monolayer (SAM) of octadecyltrichlorosilane (OTS, $CH_3(CH_2)_{16}CH_2SiCl_3$). Low surface energy of end group (CH_3) of OTS molecules is expected not only to modify the energy balance at the interface of the solid structure, the lubricant, a foreign liquid, and air, but to improve the structure's affinity for the lubricant (Wong et al., 2011). Ideally, OTS–SAM has a few nanometer thickness and strong bond (siloxane bond) with the substrate thus neither deterioration of the original profile of the nanostructure nor shortening of lifetime is expected. Vapor deposition, solution deposition, and contact printing are typical deposition methods for the modification (Wasserman et al., 1989, Kanamori et al., 2008). Solution deposition is preferable because of its simplicity and the scale extension ability. However such modification for high AR nanostructures has not been necessarily discussed. Compared with low AR structures, high AR structures are so flexible that deflection due to the meniscus attraction occur more frequently. In addition, it may be more difficult for OTS solution (of course, OTS molecules) to infiltrate into the structures with deep and narrow spaces especially at the bottom areas of the nanopores, so some areas on the surfaces may be coated by multilayer of OTS and other areas may not be coated by OTS. This problem affects to hydrophobicity of the modified surfaces, their affinity with the lubricant and it depends on OTS concentration and dipping time for reaction. Thus studying effect of the modified conditions on hydrophobicity of the modified surfaces is necessary to find the optimal condition.

This paper aims to clarify the applicability of particle mask and MACE to the fabrication of high AR micro-/nano-pore structures. The suitable condition for surface modification of such structures will be made clear. Finally, the effects of structural design and surface modification on the lubricant retention will be discussed.

2. Liquid-infused-type self-cleaning surfaces and functional lifetime

Conventional approach of self-cleaning surfaces with fine structure and/or low surface energy material coating is not enough for facile movement of low surface tension liquid drops (Fig. 1a). The drops fill in the vacant spaces easily and can't slide on the solid surface (Wenzel state, (Wenzel, 1936)). There have been two main solutions for this problem. The first solution is a special design of fine structure with local surface curvature (re-entrant morphology), solid-type self-cleaning surfaces (Fig. 1b). Here the local curvature is considered as the third parameter beside the texture and the low surface energy layer. Thus the drops are kept stably in the Cassie state (Cassie and Baxter, 1945) and slide on the surface with a small inclined angle (sliding angle, SA) (Kota et al., 2014, Liu and Kim, 2014). Wong et al. (2011) originally proposed another solution, structure surfaces (conventional design) are infused with a special liquid or liquid-type self-cleaning surfaces (Fig. 1c). This intermediate layer is the most important part of the surfaces, and their design guidelines derived from requirements for the layer. These requirements include (1) the infused liquid must infiltrate into and strongly adhere the substrate to produce a uniform layer, (2) the infused liquid (B) and foreign liquid (A) dropped on the surfaces must be immiscible, and (3) the infused layer must be not displaced by the foreign liquid. The first requirement is satisfied by using fine structures (large surface area), low surface energy layer (hydrophobicity, good chemical affinity) and the low surface tension liquid for easy infusion. Perfuoropolyether (PFPE, $F\text{-}(CF(CF_3)\text{-}CF_2\text{-}O)_n\text{-}CF_2CF_3$), lubricant of vacuum pumps, with low surface tension and immiscibility with many kinds of liquids, is usually used to satisfy the second requirement (Wong et al., 2011, Daniel et al., 2013, Zhang et al., 2014). The surface energy balance at the interface of the lubricant, foreign liquids, fine structures, and air is critical for the third requirement. The quantitative conditions can be given by Eq. (1) and Eq. (2) (Wong et al., 2011):

$$R\left(\gamma_B\cos\theta_B-\gamma_A\cos\theta_A\right)-\gamma_{AB}>0 \tag{1}$$

$$R\left(\gamma_B\cos\theta_B-\gamma_A\cos\theta_A\right)+\gamma_A-\gamma_B>0 \tag{2}$$

where γ_A and γ_B are the surface tensions for the foreign liquid and the lubricant, γ_{AB} is the interfacial tension at the

liquid-lubricant interface, θ_A and θ_B are the equilibrium contact angles of the foreign liquid and the lubricant on a flat solid surface, and R is the roughness factor (the actual surface area per the projected surface area). From these equations, conditions of surface roughness (R) and surface energy, that affects to factors of $cos\theta_A$ and $cos\theta_B$, to obtain the balance can be given when the lubricant (γ_B) and the foreign liquid (γ_A) are chosen. Next section will show experimental processes for fabrication of fine structures and surface modification.

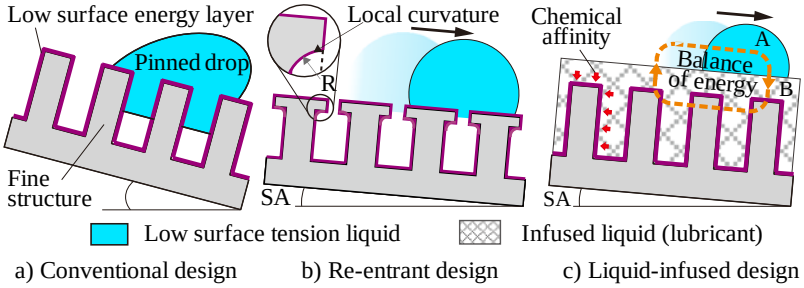

Fig. 1 Progress in the self-cleaning surface design for facile movement of low surface tension liquid drops. a) A conventional design which combines microscopic structures and low surface energy coating mimicking lotus leaf has pinning of the drops. b) A re-entrant type design requires complex manufacturing processes because of having overhang cross-sectional profile. c) A liquid-infused design has an intermediate lubricant layer to separate solid structure and the drops (Kota et al., 2014, Liu and Kim, 2014, Wong et al., 2011).

The initial performance of liquid-infused-type self-cleaning surfaces has been evaluated by measuring sliding angle or contact angle (CA) hysteresis (the difference between advancing CA and receding CA) of various liquid drops. However, evaluation of the long-term performance has been hindered by the absence of a unified definition of lifetime of liquid-infused-type self-cleaning function, the absence of a standardized test method and having different criteria for the evaluation. The liquid-infused surfaces operated against various stimuli such as high shear stress to remove the lubricant (Kim et al., 2013), high temperature to increase the evaporation rate of lubricant (Wong et al., 2011) or to reduce the surface tension of the foreign liquids (Daniel et al., 2013). Then functional comparison or changing of SA is usually used as the criterion to conclude the function has preserved for long time. Therefore we proposed a simple definition for the lifetime, which is the duration of the self-cleaning function. The duration will finish when droplets of a specified liquid can't slide on the surfaces at a specified inclined angle. In this work, diethylene glycol (a low surface tension liquid) will be used and the inclined angle of 20° will be set. The test method will be shown later (Section 3.3).

3. Experimental procedure

3.1 Structuring process

Figure 2 shows a schematic of a fabrication procedure. First, silica particles were self-assembled on a silicon substrate using dip coating method to produce a monolayer (Kanamori et al., 2008, Nishio et al., 2014, Moronuki et al., 2016b). A gold layer was then deposited using physical vapor deposition (PVD), originally used for scanning electron microscope (SEM) observation coating. PVD was chosen because it can easily deposit a pure and porous gold layer in short time. The substrate was etched in a solution of hydrofluoric acid (HF), hydrogen peroxide (H_2O_2), and ethanol (C_2H_5OH). Ethanol was added to enhance the stability of the Au layer in the etchant and to improve the controllability of etching rate (Moronuki et al., 2016b). Table 1 shows the detail conditions for the process. Pattern size of Au islands depends on particle diameter thus ϕ10 μm and ϕ1 μm silica particles were used for the fabrication of micropore structures and nanopore structures respectively. To obtain monolayer of particles in a wide area, different dip-coating conditions (drawing up speed, angle) were used for silica particles with different sizes because of dispersed difference of the particles in their suspensions. Etching time was changed for various aspect ratios and etching rate was calculated.

3.2 Surface modification

A clean, dry, and rich hydroxyl surface is necessary to obtain uniform self-assembled monolayer (SAM) of OTS. Thus the Au layer, the residue of the MACE process, was etched using a solution of hydrochloric acid and nitric acid (Fig. 3a). Next step is hydroxylation (Fig. 3b). In this case, piranha treatment was used to clean and to produce hydroxyl groups on the structured surfaces. Because of using liquid environment for the hydroxylation, stiction phenomenon, the free-ends of nanostructures get together due to the meniscus attraction of the rinse solution during the evaporation process, often occurs (Chang et al., 2009, Moronuki et al., 2016b). This problem was reduced by using the same method

as fabrication of high AR structures (Balasundaram et al., 2012, Moronuki et al., 2016b). In process of rinsing, the wet substrate taken from the piranha solution was dipped in an ethanol container for solvent exchange, the substrate was then put on a hot plate to control drying step (Fig. 3c). Finally, the substrate was dipped in a solution of OTS and anhydrous toluene in certain time and exceeded OTS was removed by anhydrous toluene (Fig. 3d). To control humidity that affects to formation of OTS monolayer, this step was done in a glove box purged with dry N_2 gas. Table 2 shows the experimental conditions for the surface modification. In this work, OTS concentration of 3 wt% was chosen and the dipping time was changed from 20 min to find suitable conditions based on our previous studies (Kanamori et al., 2008, Nishio et al., 2014). A high AR nanopore structure was used to estimate effect of the dipping time.

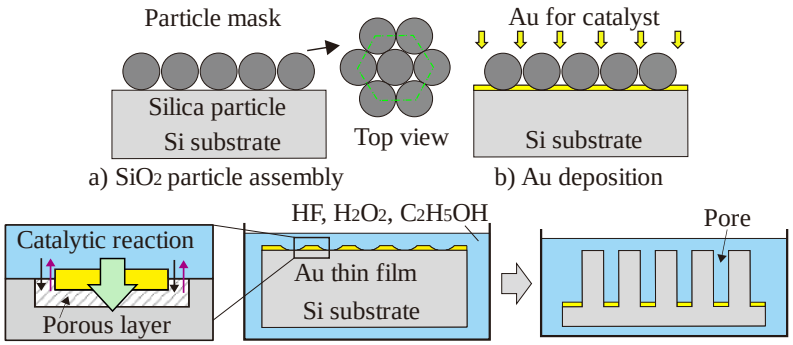

Fig. 2 A fabrication procedure of micro-/nano-pore structures. a) A particle mask was produced via self-assembly of silica particles on a silicon substrate (right inset is a top view of the particle mask). b) A gold layer was then deposited through the particle mask for Au patterning. c) Finally, the substrate was dipped in the etchant. Left schematic shows the mass transport model of MACE when using metal thin film for catalyst (Geyer et al., 2012).

Table 1 Structuring conditions.

Substrate	Material, size	Silicon, 10 mm×10 mm	
Self-assembly	Particles	Silica ϕ 10 μm	Silica ϕ 1 μm
	Solvent	Ultrapure water	
	Concentration	10 wt%	5 wt%
	Drawing up speed, angle	0.5 mm/s, 60°	1 mm/s, 45°
Au layer thickness, Deposition method		20 nm, PVD	
MACE conditions	Etchant	HF:H_2O_2:C_2H_5OH=3:1:6	
	Temperature	20 °C	
	Etching time	5, 10, 15, 20 min	

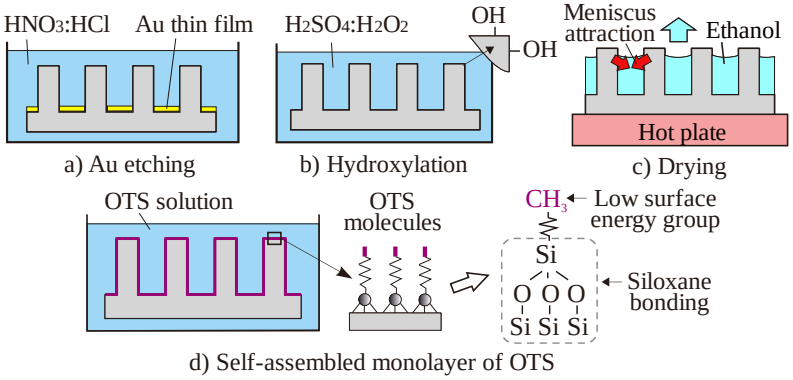

Fig. 3 Surface modification of high AR nanostructures. a) The residual Au layer was removed by dipping of the substrate in a solution of nitric acid and hydrochloric acid. b) Next, the substrate was dipped in a solution of sulfuric acid and hydrogen peroxide for cleaning and hydroxylation. c) After rinsing in ethanol, the substrate was put on a hot plate to dry under control. d) Finally, the substrate was dipped in the OTS solution for OTS–SAM formation.

Table 2 Detail conditions for surface modification.

Au etching	Solution	HNO_3:HCl=1:3
	Time	2 min
Hydroxylation	Piranha solution	H_2SO_4:H_2O_2=3:1
	Time, Temperature	2 hour, 70 °C
	Rinsing, Drying	Ethanol, 60 °C
OTS deposition	OTS solution	3 wt%, Anhydrous toluene
	Time	20 min–480 min
	Washing solution	Anhydrous toluene

3.3 Evaluation of lifetime

In this work, Krytox® 103 (a PFPE liquid) and diethylene glycol (DEG) were used as the infused liquid and the foreign liquid respectively. Sudan I (Sigma Aldrich), a dye with orange color, was mixed with DEG to enhance the contrast of observation images. Before the evaluation, the modified surface was infused with Krytox® 103 (100 µl/sample) via the capillary force. The surface was kept for 4 hours (at room condition) to obtain full wetting and exceeded lubricant was removed to produce a stable and uniform lubricant layer. The initial thickness of the lubricant was kept constant by controlling the volume of lubricant put over the structured area. The weight of the lubricant was measured with a high resolution electric balance and the volume was estimated dividing by its density. The thickness was assumed constant over the specimen. Ideally, there was no difference in the initial thickness of lubricant between low AR and high AR structures. Table 3 summarizes all liquids used in this work for their scope of use and surface tension.

An original set up, that examines the lifetime against a load assuming rainfall, was used for the evaluation due to the lack of standardization. Figure 4 shows the schematic. A base used to set samples and a charge-coupled device (CCD) camera used to take top view images were set perpendicularly. A cup used to pour liquids on the samples was fixed to the base. These parts were attached on a rotary stage. This stage and the camera were controlled by a personal computer. At the initial position of this stage, the sample and the liquid cup were set vertically (position 1). The dash procedure includes (1) rotate the stage 110° to position 2 (the surface of sample has an inclined angle of 20°) therefore the liquid (DEG, 5 ml) in the cup is poured on the sample, (2) take a top image, and (3) return to the initial position. The procedure was repeated to find the DEG residue and the lifetime was the number of dash at which the residue started to occur. The coverage of DEG residue was calculated by using an image processing software, ImageJ. The original images were filtered and converted to binary images, the coverage was then calculated.

Table 3 Summary of all liquids used in this study.

Liquid	Scope		Surface tension (mN/m)
Krytox® 103	Infusion		15–20
Water		Wettability evaluation	72.8
DEG	Dash		44.8
Ethanol	Rinsing		22.1
Anhydrous toluene	Surface modification		28.4

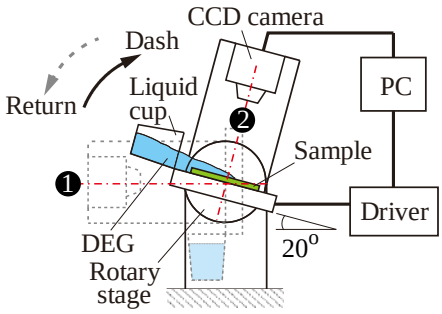

Fig. 4 Set up for evaluation of residue of dash liquid that expresses lifetime of function.

4. Results and discussion

4.1 High aspect ratio micro-/nano-pore structures

Figure 5 shows the results of the structuring process. The silica particles were assembled in a hexagonally packed structure over a wide area (Fig. 5a). In Fig. 5b, the Au pattern was confirmed by a scanning electron microscope (SEM) image. For observation convenience, the silica particles were removed by ultrasonic cleaning. Finally, well-ordered micro-/nano-pore arrays were obtained with hexagonal patterns correspond with ϕ10 µm or ϕ1 µm silica particles (Fig. 5c, d). These were the evidences for capability of this fabrication process to produce both micropore structures and

nanopore structures. The cross-sectional view in Fig. 5d shows clearly a high aspect ratio (AR=14) nanopore structure. Based on height of structures (etched depth) and pore diameter, aspect ratio was calculated. Isolated areas of pores were extracted from the top view SEM images by using the image processing software (ImageJ), the diameter distribution was then calculated (Fig. 5d, right side). Ideally, the pore pitch is equal to the particle diameter and the pore diameter corresponds to the pattern size of the deposited Au layer which is roughly proportional to the particle diameter. In this work, the particle diameter was changed to control the pore diameter and the pitch while the Au thickness was fixed. Because the final aim is the long-term lubricant retention, we focused on fabrication of nanopore structures and controllability of their aspect ratio. Fig. 5e shows the relation between etching time and etched depth (height of structure), the etching rate was found around 0.7 μm/min. The highest aspect ratio was 30 (the height was approximate 15 micron). Hence etching time is the dominant and effective factor to control the aspect ratio of the nanopore structures.

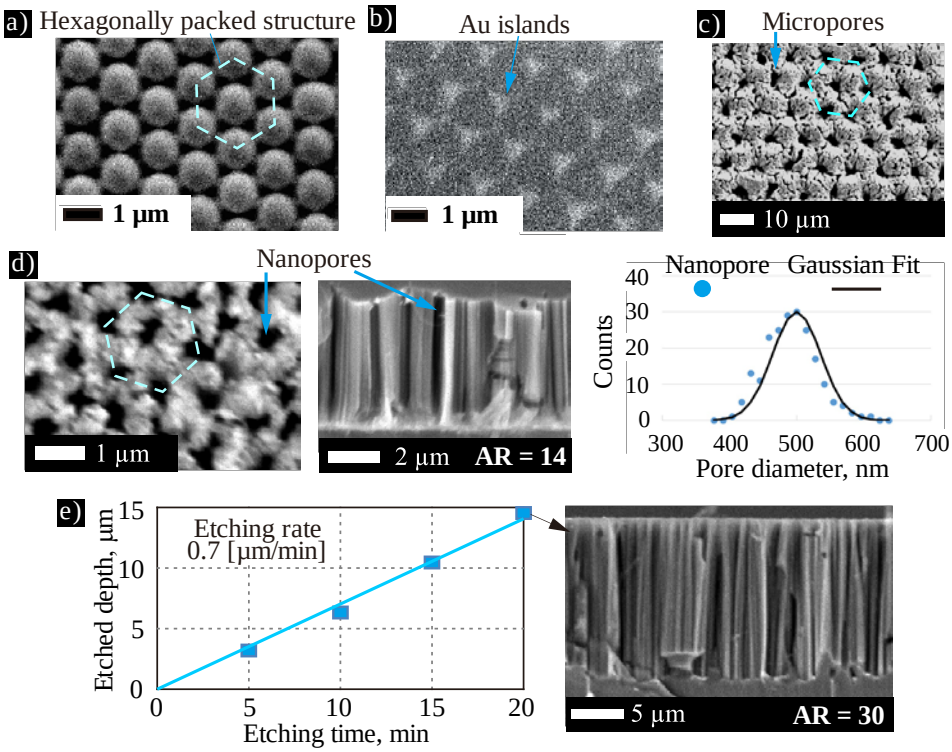

Fig. 5 High aspect ratio micro-/nano-pore structures. a) A mask of silica particles (ϕ1 μm). b) Regular pattern of Au layer. c) A top view of micropore structure. d) A top view and a cross-sectional view of a nanopore structure (left, center side) and diameter distribution of pores (right side). e) Relation between etching time and etched depth (using ϕ1 μm silica particle) and a cross-sectional view of the nanopore structure with the highest AR.

4.2 Liquid-infused nanopore surfaces and their functional lifetime

After the surface modification, nanopore surfaces were infused with the lubricant. Figure 6 shows (a) schematic representations of lubricant thickness and infiltrated depth of the lubricant in nanopores with respect to different aspect ratios assuming trapped air was existed in high AR structures and (b) the relation between the coverage of the DEG residue on the corresponding surfaces and number of dash. The low aspect ratio (AR = 6) structure only retained the lubricant in short time, proved by the coverage, nearly 10 percent after 100 times of dash. Thus the corresponding surface had short functional lifetime, 20 times of dash. While the high aspect ratio structures (AR = 14, or AR = 30) hold the lubricant tight and the corresponding surfaces had long functional lifetime, 200 times of dash or longer 400 times of dash respectively. The inset images are the top views of the surface with the aspect ratio of 14. The pinning of DEG drops was explained through the corresponding schematic. The lubricant layer was removed partially thus the solid structure was exposed and contacted directly with the drops.

It was confirmed that the higher AR showed the longer lifetime. However, no evidences have been shown that the lubricant fills up the whole vacant spaces in the structures. If air was trapped under the lubricant layer, the effect of AR would be limited by the lubricant infiltrated depth (Fig. 6a). Here a simple method was used to verify the issue. There was the appearance difference of the nanopore (AR = 30) surface with and without the lubricant when dipping in water

(Fig. 7). Without lubricant, the sample looked white and bright that is evidence of the trapped air (Zimmermann et al., 2008, Artus et al., 2012). On the other hand, the infused sample looked brown (resembling the original color of the solid surface). The difference (no bright color) is considered as the occurrence of the trapped lubricant in the vacant spaces of the nanopore structure and no existence of the trapped air. The evaluation based on visual judgment of color might be too simple and more accurate measurement should be considered. However, it is not easy to confirm the existence of the lubricant at the bottom of nanopores with diameter of submicron and depth of 15 micron.

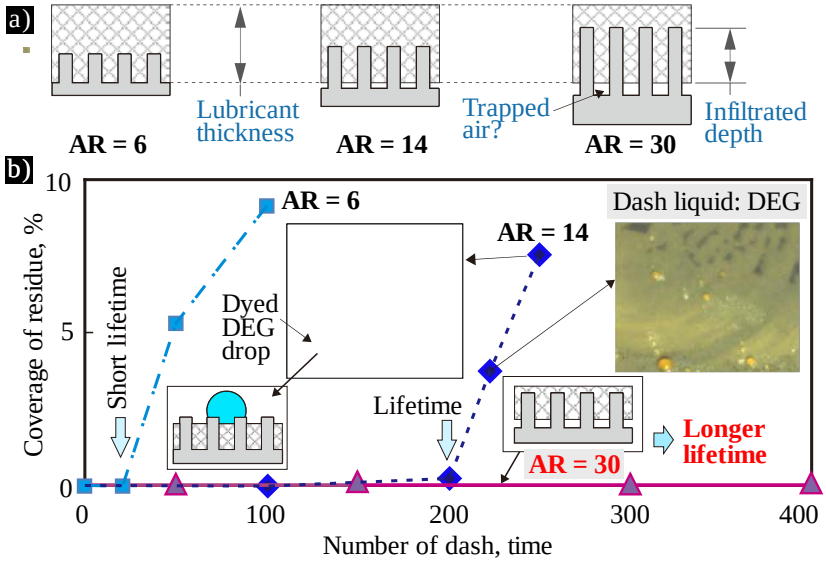

Fig. 6 Lifetime evaluation. (a) Schematic representations of lubricant thickness and infiltrated depth of the lubricant in nanopores with respect to different aspect ratios assuming trapped air existed in high AR structures. (b) Relation between the coverage of DEG residue on the liquid-infused nanopore surfaces and number of dash. The surface with AR of 6 had short lifetime, around 20 dash times. After around 200 dash times, the lubricant layer was removed partially and the solid structure (AR=14) was exposed thus DEG drops were pinned on the surface (2 top views and the corresponding schematic). With high AR (AR=30), the surface had longer functional lifetime.

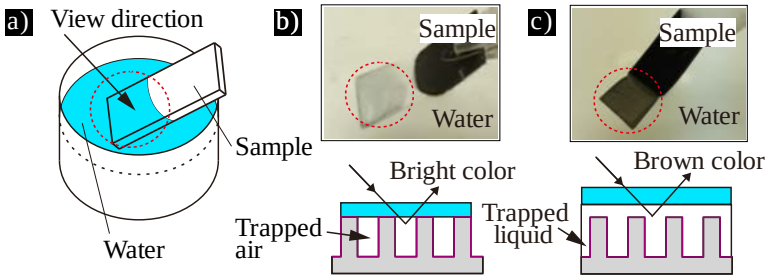

a) Schematic b) Nanopore structure c) Liquid infused structure

Fig. 7 Different appearances of nanopore (AR of 30) surfaces without and with the infused lubricant when dipping in water. a) Schematic. b) Without the lubricant, the sample looked white and bright due to trapped air explained by corresponding schematic shown below. c) With the lubricant, the sample looked brown due to trapped liquid explained by corresponding schematic shown below, no air was trapped.

4.3 Self-assembled monolayer for high aspect ratio nanopore structures

The effect of dipping time on hydrophobicity of the structured (AR of 21) surface was investigated by measuring the contact angle (CA) of water droplets on the modified surfaces (Fig. 8). When the dipping time was 20 minutes, the CA of 138° was the smallest angle (the top left photo). After 40 minute dipping time, the CA increased up to 152° (the top center photo). With the continuous increase of the dipping time, the CA decreased slightly and had a steady value around 150°. The reason may be considered as OTS–SAM was formed partially on the surface with the dipping time of 20 minutes. Extending the dipping time, the coverage of OTS-SAM increased and the optimal hydrophobicity was obtained (40 minutes). Continuous extending of the dipping time (longer than 40 minutes) might result in continued deposition of

OTS molecules and the hydrophobic layer on the top part of the nanopores was multilayer, not monolayer. The additionally deposited material might change the morphology of the high AR nanopore structure and/or this material was not well oriented so as to expose the hydrophobic group (CH_3) on the top of the surface. Thus the contact angle (and the affinity with the lubricant) decreased. There was no evidence shown in the result due to measured difficulty of OTS-SAM in the deep nanopores. The trend of CA decrease is different from that of a non-structured surface, the additionally deposited OTS enhanced roughness of the surface, so CA increased (Wang and Lieberman, 2003). The top right image in Fig. 8 is the top view of the high AR structure after the modification (40 minute dipping time), the morphology of pore structure was remained. Thus surface tension of OTS solution had insignificant effect in this case.

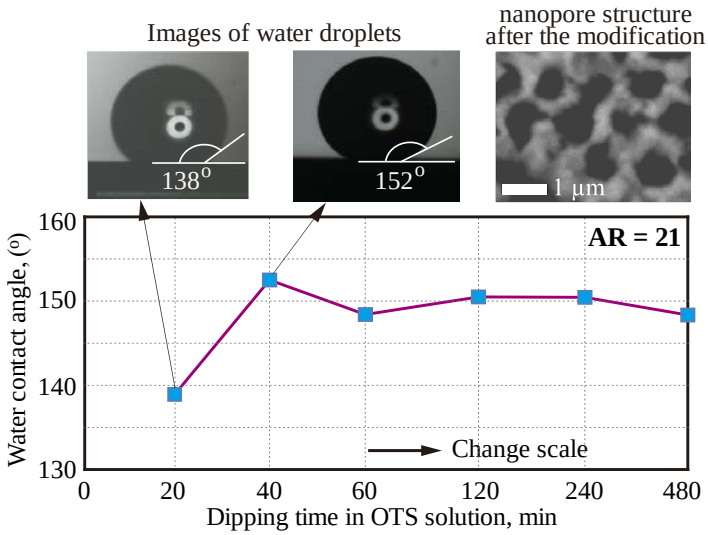

Fig. 8 Effect of dipping time on water contact angles of the modified surface with aspect ratio of 21 (droplet volume=10 μl). Inset: photos of water droplets on the modified surfaces with dipping time of 20 min and 40 min (left side, center), a top view of the nanopore structure (AR=21) after 40 min dipping time (right side).

4.4 Self-cleaning performance

Effects of aspect ratio of the nanopore structures and liquids with different surface tension on initial self-cleaning performance of the liquid-infused surfaces were evaluated by measuring sliding angles of droplets of the liquids (water, DEG, and ethanol) on the surfaces. Fig. 9a shows the relation between sliding angle of DEG drops and aspect ratio. With AR from 6 to 30 (high roughness factor, R), these surfaces had almost same initial performance. Here the AR had insignificant effect on the performance because the lubricant layer was kept stably in all cases. Whereas a DEG drop didn't slide down in case of without structure ($R = 1$) because of having an unstable lubricant layer (Section 2, Eq. (1) and Eq. (2)). Fig. 9b shows the sliding angle of various liquids on the liquid-infused surface (AR=21). Droplets of water and DEG could slide easily on the surface with very small tilting angles. The left insets show the movement of a water drop on the surface that had a nearly horizontal position. However, a drop of ethanol spread as shown in the right insets (dot circles) and could not slide down. In this case, the lubricant layer was unstable and removed from the surface. The reason can be considered as the unbalance of surface energy at the interface (Section 2, Eq. (1) and Eq. (2)) due to very low surface tension of ethanol (Table 3). To overcome this issue, other silanes with lower surface tension end groups (e.g. CF_3) should be used for the surface modification (Wong et al., 2011, Zhang et al., 2014).

5. Conclusions and future works

Combination of self-assembly of particles and MACE could produce well-ordered, high aspect ratio micro-/nano-pore structures. The surfaces of these structures were modified successfully using self-assembled monolayer of OTS. The high aspect ratio nanopore structures could keep the lubricant against large number of dash that showed the durable lubricant retention ability. The liquid-type self-cleaning surfaces with longer functional lifetime were obtained.

Quantitative evaluation of the liquid penetration depth is one of the future problems. Another one is the scale extension of the structuring area. Transfer print may be a solution to deposit noble metals that eliminates the dependence of this step on the vacuum process. Durable improvement against mechanical contact should be considered.

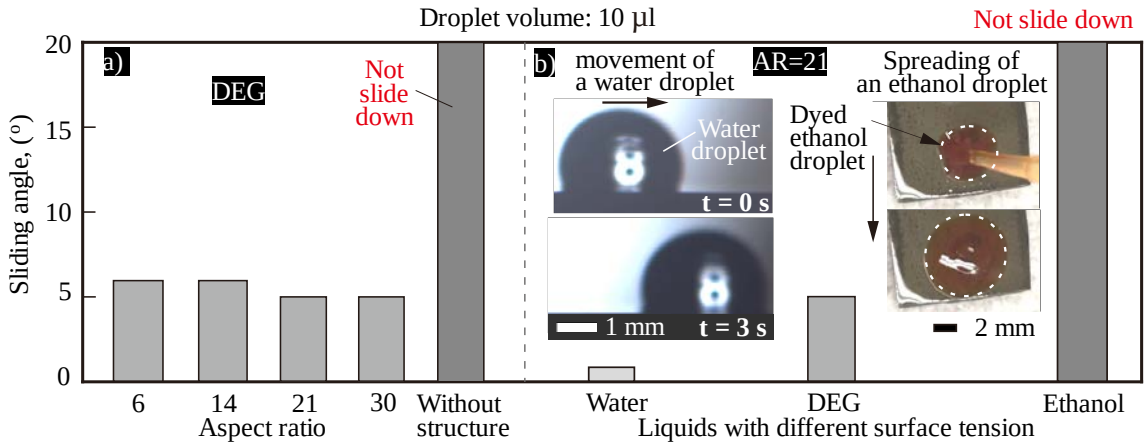

Fig. 9 Self-cleaning performance of the lubricant-infused high AR nanopore surfaces with (a) various AR and (b) various liquids. (a) When using DEG for the evaluation, the surfaces with AR from 6 to 30 had almost same initial performance, whereas a DEG drop didn't slide down in case of without structure. (b) With AR of 21, the surface had high performance when using water or DEG, SA of 1° or 5° respectively. However, an ethanol droplet spread widely and didn't slide down due to very low surface tension of ethanol.

References

Artus, G. R. J., Zimmermann, J., Reifler, F. A., Brewer, S. A. and Seeger, S., A superoleophobic textile repellent towards impacting drops of alkanes, Applied Surface Science, Vol.258, No.8 (2012), pp.3835–3840.

Aruga, D., Kaneko, A. and Moronuki, N., Design of quick–dry surface using structured surface, Journal of Advanced Mechanical Design, System, and Manufacturing, Vol.2, No.4 (2008), pp.773–782.

Balasundaram, K., Sadhu, J. S., Shin, J. C., Azeredo, B., Chanda, D., Malik, M., Hsu, K., Rogers, J. A., Ferreira, P., Sinha, S. and Li, X., Porosity control in metal-assisted chemical etching of degenerately doped silicon nanowires, Nanotechnology, Vol.23, No.30 (2012), pp.305304.

Cao, L., Jones, A. K., Sikka, V. K., Wu, J. and Gao, D., Anti-icing superhydrophobic coatings, Langmuir, Vol.25, No.21 (2009), pp12444–12448.

Cassie, A. B. D. and Baxter, S., Large contact angles of plant and animal surfaces, Nature, Vol.155, No.3923 (1945), pp.21–22.

Chang, S. W., Chuang, V. P., Boles, S. T., Ross, C. A and Thompson, C. V., Densely packed arrays of ultra-high-aspect-ratio silicon nanowires fabricated using block-copolymer lithography and metal-assisted etching, Advanced Functional Materials, Vol.19, No.15 (2009), pp.2495–2500.

Daniel, D., Mankin, M. N., Belisle, R. A., Wong, T. S. and Aizenberg, J., Lubricant-infused micro/nano-structured surfaces with tunable dynamic omniphobicity at high temperatures, Applied Physics Letters, Vol.102 (2013), pp.231603–1.

Epstein, A. K., Wong, T. S., Belisle, R. A., Boggs, E. M. and Aizenberg, J., Liquid-infused structured surfaces with exceptional anti–biofouling performance, Proceedings of the National Academy of Sciences of the United States of America, Vol.109, No.33 (2012), pp.13182–13187.

Geyer, N., Fuhrmann, B., Huang, J., Boor, J., Leipner, H. S. and Wener, P., Model for mass transport during metal-assisted chemical etching with contiguous metal films as catalyst, The journal of physical chemistry C, Vol.116, No.24 (2012), pp.13446–13451.

Huang, J., Fang, H. and Zhu, J., Fabrication of silicon nanowire arrays with controlled diameter, length, and density, Advanced Materials, Vol.19, No.5 (2007), pp.744–748.

Huang, J., Geyer, N., Werner, P., Boor, J. D. and Gosele, U., Metal-assisted chemical etching of silicon: a review, Advanced Materials, Vol.23, No.2 (2011), pp.285–308.

Kanamori, Y., Kaneko, A., Moronuki, N. and Kubo, T., Self-assembly of fine particles on patterned wettability in dip coating and its scale extension with contact printing, Journal of Advanced Mechanical Design, System, and Manufacturing, Vol.2, No.4 (2008), pp.783–791.

Kim, P., Kreder, M. J., Alvarrenga, J. and Aizenberg, J., Hierarchical or not? Effect of the length scale and hierarchy of the surface roughness on omniphobicity of lubricant-infused substrates, Nano Letters, Vol.13, No.4 (2013), pp.1793–1799.

Kota, A. K., Kwon, G. and Tuteja, A., The design and applications of superomniphobic surfaces, NPG Asia Materials, Vol.6 (2014), pp.1–16.

Kreder, M. J., Alvarrenga, J., Kim, P. and Aizenberg, J., Design of anti–icing surfaces: smooth, textured or slippery?, Nature Reviews Materials, Vol.1 (2016), pp.1–15.

Liu, T. L and Kim, C. J., Turning a surface superrepellent even to completely wetting liquids, Science, Vol.346, No.6213 (2014), pp.1096–1100.

Moronuki, N., Functional texture design and texturing processes, International Journal of Automation Technology, Vol.10, No.1 (2016), pp.4–15.

Moronuki, N., Phan, N. and Keyaki, N., Fabrication of high aspect ratio silicon nanostructure with sphere lithography and metal-assisted chemical etching and its wettability, International Journal of Automation Technology, Vol.10, No.6 (2016), pp.971–976.

Nishio, M., Moronuki. N. and Abasaki, M., Fabrication of patterned Ag and Au inverse opal structures through repeated self-assembly of fine particles, International Journal of Automation Technology, Vol.8, No.5 (2014), pp.755–760.

Peng, K., Zhang, M., Lu, A., Wong, N-B., Zhang, R. and Lee, S-T., Ordered silicon nanowire arrays via nanosphere lithography and metal-induced etching, Applied Physics Letters, Vol.90, (2007), pp.163123–3.

Tuteja, A., Choi, W., Ma, M., Mabry, J. M., Mazzela, S. A., Rutledge, G. C., McKinley, G. H. and Cohen, R. E., Designing superoleophobic surfaces, Science, Vol.318, No.5856 (2007), pp.1618–1622.

Wang, Y. and Lieberman, M., Growth of ultrasmooth octadecyltrichlorosilane self-assembled monolayers on SiO_2, Langmuir, Vol.19, No.4 (2003), pp.1159–1167.

Wasserman, S. R., Tao, Y. T. and Whitesides, G. M., Structure and reactivity of alkylsiloxane monolayers formed by reaction of alkyltrichlorosilanes on silicon substrates, Langmuir, Vol.5, No.4 (1989), pp.1074–1087.

Wenzel, R. N., Resistance of solid surfaces to wetting by water, Ind. Eng. Chem., Vol.28, No.8, pp.988–994.

Wong, T. S., Kang, S. H., Tang, S. K. Y., Smythe, E. J., Hatton, B. D., Grinthal, A. and Aizenberg, J., Bioinspired self–repairing slippery surfaces with pressure–stable omniphobicity, Nature, Vol.477, No.7365 (2011), pp.443–447.

Zhang, J., Wu, L., Li, B., Li, L., Seeger, S. and Wang, A., Evaporation–induced transition from nepenthes pitcher–inspired slippery surfaces to lotus leaf–inspired superoleophobic surfaces, Langmuir, Vol.30, No.47 (2014), pp.14292–14299.

Zimmermann, J., Reifler, F. A., Fortunato, G., Gerhardt, L. and Seeger, S., A simple, one-step approach to durable and robust superhydrophobic textiles, Advanced Functional Materials, Vol.18, No.22 (2008), pp.3662–3669.